THE JOURNAL OF PHYSICAL CHEMISTRY Letters

pubs.acs.org/JPCL Letter

Long Persistent Luminescence Enabled by Dissociation of Triplet Intermediate States in an Organic Guest/Host System

Leixin Xiao,[@] Zhiwei Wang,[@] Chunfeng Zhang,* Xiaoyu Xie, Haibo Ma, Qian Peng, Zhongfu An, Xiaoyong Wang, Zhigang Shuai, and Min Xiao

Cite This: *J. Phys. Chem. Lett.* 2020, 11, 3582−3588 Read Online

ACCESS | Metrics & More | Article Recommendations | Supporting Information

ABSTRACT: Organic guest/host systems with long persistent luminescence benefiting from the formation of a long-lived charge-separated state have recently been demonstrated. However, the photogeneration mechanism of such key charge-separated states remains elusive. Here, we report the identification of intermediate triplet states with mixed local excitation and charge-transfer character that connect the initial photoexcited singlet states and the long-lived charge-separated states. Using time-resolved optical spectroscopy, we observe the intersystem crossing from photoexcited singlet charge-transfer states to triplet intermediate states on a time scale of ∼52 ns. Temperature-dependent measurements reveal that the long-lived triplet intermediate states ensure a relatively high efficiency of diffusion-driven charge separation to form the charge-separated state responsible for LPL emission. The findings in this work provide a rationale for the development of new LPL materials that may also improve our understanding of the mechanism of photon-to-charge conversion in many organic optoelectronic devices.

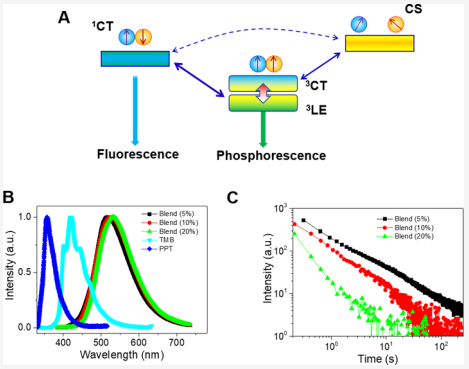

Organic molecules displaying long persistent luminescence (LPL) are attracting rapidly growing interest because of their potential applications as large scale and flexible paints, biomarkers, and display devices.[1−9] Conventionally, phosphorescence from a triplet excited state is the long-lived emission component from organic luminogens.[10−16] Stabilizing the triplet state by different strategies can provide the ultralong phosphorescence with a lifetime up to the order of seconds at room temperature.[8,17−26] Organic guest/host systems with electronic donors and acceptors have recently been proposed to further extend the persistence of luminescence.[27−29] This strategy holds the potential to dramatically enlarge the family of LPL materials by combining different donors and acceptors.

In the guest/host systems, the intermolecular charge-separated (CS) states have been suggested to account for the exceptionally long-lived emission arising from the recombination of encountered electrons and holes. The CS state is composed of a radical cation of the donor and radical anion of the acceptor. However, the formation mechanism of such a CS state in organic LPL materials remains elusive. The photogeneration mechanism for charge separation in donor/acceptor blends in organic photovoltaic (OPV) materials has been intensively studied.[30] In the widely studied polymer/fullerene systems, photon absorption creates local excitations in the donor, which form interfacial charge-transfer states with singlet character (^{1}CT) through an electron-transfer process.[30] The ^{1}CT states then dissociate into the CS states of free charges.[30] However, the lifetime of such a CS state is limited to the time scale of microseconds or shorter because of the bimolecular recombination in OPV blends.[30] Efficient LPL has been observed on a much longer time scale,[27−29] suggesting that LPL in organic guest−host systems has a different charge separation mechanism.

In this work, we study the mechanism responsible for LPL in a model guest/host system consisting of the electron-donating molecule *N*,*N*,*N*′,*N*′-tetramethylbenzidine (TMB) and electron-accepting molecule 2,8-bis(diphenylphosphoryl)dibenzo[*b*,*d*]thiophene (PPT) by probing the dynamics of photoexcited carriers in TMB/PPT blends on time scales from subpicoseconds to seconds using transient absorption (TA) spectroscopy. We identify a new channel for photogeneration of the CS states through long-lived triplet intermediate states. The ^{1}CT states generated by photon absorption undergo the process of intersystem crossing (ISC) to form intermediates (Figure 1A) of mixed locally excited triplet states (^{3}LE) of TMB and triplet CT states (^{3}CT). The intermediate triplet states are long-lived, which allows the efficient formation of CS states driven by the diffusion of radical anions in the PPT matrix (Figure 1A), enabling the LPL in the TMB/PPT

Received: March 20, 2020
Accepted: April 15, 2020
Published: April 17, 2020

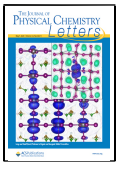

https://dx.doi.org/10.1021/acs.jpclett.0c00880
J. Phys. Chem. Lett. 2020, 11, 3582−3588

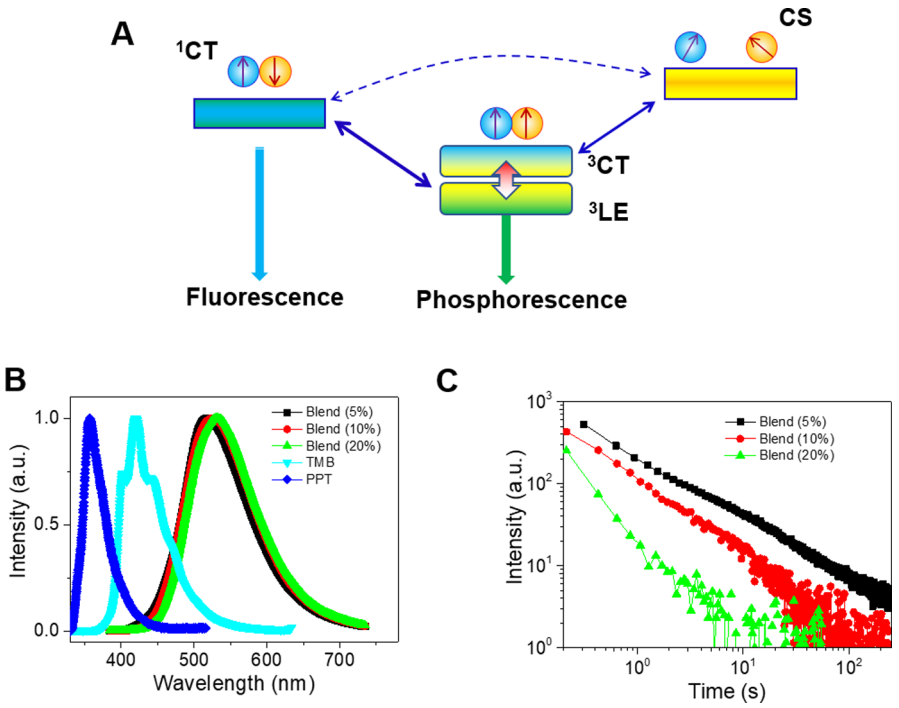

Figure 1. Triplet state-mediated LPL in TMB/PPT blends. (A) Diagram of charge separation through intermediate triplets of mixed ^{3}LE and ^{3}CT states. (B) Photoluminescence spectra of blend films with different doping levels of TMB and neat films of TMB and PPT. (C) Double-logarithmic plot of the emission decay profile of the same blend films at room temperature.

blends. The identification of such a triplet channel for long-lived charge separation may guide the search for high-performance LPL emitters and spur the development of organic optoelectronic devices using the triplet channel for photon-to-charge conversion.

Emission spectra from TMB/PPT blends with different molar ratios of TMB are compared with those of neat films of TMB and PPT in Figure 1B. The emission wavelengths of the blend films are much longer than those of the neat films of TMB and PPT, which is consistent with the involvement of CT states. The longer persistence of photoluminescence (PL) emission was observed for the samples with a lower ratio of TMB (Figure 1C), implying that carrier diffusion plays an important role in the LPL of the blends.[27]

We perform transient optical measurements to study the carrier dynamics from primary excitation to LPL emission. Figure 2 shows the experimental data obtained for a blend sample with a 10 mol % ratio of TMB on different time scales. In the initial stage, photoexcitation in the TMB/PPT blend causes the formation of the ^{1}CT state as observed in the femtosecond-resolved TA spectra. As a consequence of charge transfer, the excited-state absorption (ESA) features of the blend film (Figure 2) show marked differences from those in the neat TMB and PPT films (Figure S1). The ESA feature in the near-infrared region shows a red shift from 940 nm for the neat TMB film to 1050 nm for the blend (Figure 2A). ESA at 1050 nm is similar to the reported spectral characteristic of the free radical cation of TMB (TMB^+).[31] However, the TMB^+-liked ESA signal at this stage is not caused by the CS state in the blend, as suggested by the dynamics on the nanosecond time scale (Figure 2B–D). The ESA signal at 1040 nm decays exponentially with a characteristic lifetime of ~52 ns, which is independent of pump fluence (Figure S2). This result indicates that bimolecular recombination, a character of free charges of

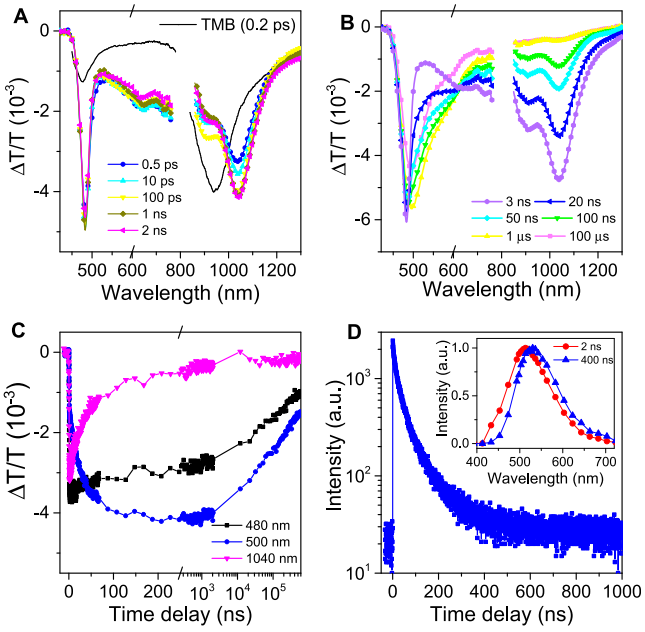

Figure 2. Dynamics of charge transfer and ISC in the TMB/PPT blend film. (A) Femtosecond-resolved and (B) nanosecond-resolved TA spectra of a 10 mol % TMB/PPT film. The TA spectrum of a neat TMB film at a delay of 0.2 ps is also shown for comparison. (C) Nanosecond-resolved kinetic curves probed at different wavelengths. Femtosecond- and nanosecond-resolved TA spectra were recorded upon pumping with femtosecond pulses at 360 nm and nanosecond pulses at 355 nm, respectively. (D) TRFL spectrum of the blend film probed at 530 nm. The inset shows the emission spectra recorded at delays of 2 and 400 ns.

the CS state, is absent. It is reasonable to assign the ESA signal to the ^{1}CT state with relatively weakly interacting TMB^+ and

https://dx.doi.org/10.1021/acs.jpclett.0c00880
J. Phys. Chem. Lett. 2020, 11, 3582−3588

PPT^{-}. The broadband nanosecond-resolved TA signal can be reproduced by the global fitting algorithm considering a spectral transfer with a lifetime of ~52 ns (Figure S3), suggesting the formation of a new excited state from the ^{1}CT state.

The new excited species exhibits an ultralong lifetime, persisting for >100 μs (Figure 2B,C), which is likely caused by the ISC from the ^{1}CT state to an intermediate triplet state. The ESA signals for the two excited species are caused by optical transitions from the ^{1}CT state to higher singlet states and from the intermediate triplet state to higher triplet states, exhibiting a dramatic spectral transfer. This assessment is supported by the time-resolved fluorescence (TRFL) spectrum (Figure 2D) recorded for the blend film, which contains a decay component with a similar lifetime of ~50 ns caused by a transition from the ^{1}CT state to a state with different spectral character (inset of Figure 2D). The wavelength of fluorescence emission from the ^{1}CT state (2 ns) is slightly shorter than that of phosphorescence (400 ns) from the intermediate triplet state (inset of Figure 2D). The involvement of a triplet intermediate is explicitly confirmed by the electron spin resonance (ESR) measurements (Figure 3A). In addition to

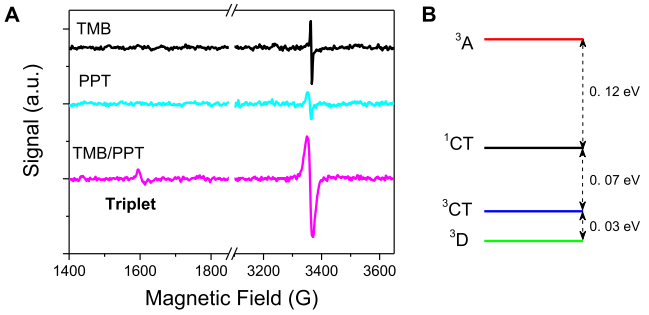

Figure 3. Triplet states generated in a photoexcited TMB/PPT blend film. (A) ESR signals of the blend film and neat films of TMB and PPT recorded at 77 K upon optical excitation at 355 nm. The wavelength of the excitation source was 355 nm. (B) Calculated energy alignment of the ^{1}CT, ^{3}CT, and triplet excitations localized at TMB (^{3}D) and PPT (^{3}A) sites for a TMB/PPT dimer configuration (Figures S4 and S5 for details).

the signal in the g = 2 region induced by radicals, a substantial signal of the triplet signature near 1600 G under photoirradiation in the g = 4 region is observed for the blend film, which is not present in the ESR spectra of the neat films (Figure 3).[32] Such a new feature strongly supports the formation of a triplet intermediate in the TMB/PPT blend film.

To study the nature of the triplet intermediate, we perform quantum chemical computations to survey the energy alignment of possibly involved triplet states (Figures S4 and S5 and Table S1).[33] In the TMB/PPT blend, the triplet states may be generated by local excitations (^{3}LE) at the sites of either TMB or PPT or by charge-transfer excitation (^{3}CT) at the donor/acceptor interface. The calculation results (Figure 3B) suggest that the ^{3}LE state of TMB and the ^{3}CT state are the two triplet states lying below the ^{1}CT state (Figures S4 and S5; see the Supporting Information for more details). The orbital types of these states are shown in Figure S4. The orbital type of the ^{1}CT state is similar to that of the ^{3}CT state but dramatically different from that of the ^{3}LE state. It should also be noted that the low-lying energy landscape would vary during the thermal fluctuations. However, our further quantum chemical calculations of various typical dimer geometries with different intermolecular distances and/or interactions from molecular dynamics simulations under room temperature still show that the ^{3}LE state of TMB and the ^{3}CT state are always located energetically below the ^{1}CT state (Table S1), supporting our model under realistic conditions. According to the El-Sayed rule, the direct ISC process between ^{1}CT and ^{3}CT states is less efficient than that between ^{1}CT and ^{3}LE states.[21,34] The experimental study of the ISC in CT excited states suggests that the ISC rate is dramatically reduced for the states with full CT character.[35] It is therefore reasonable to assign the process with a characteristic lifetime of 52 ns to the ISC process from the ^{1}CT to the ^{3}LE state at TMB. The small energy difference between the ^{3}LE state at TMB and the ^{3}CT state (Figure 3B) allows efficient conversion between these two triplet states at room temperature. These findings suggest that the triplet intermediate is probably a mixture of the ^{3}LE and ^{3}CT states, which is consistent with the result that the ESA feature was comparable to but not the same as that of the ^{3}LE state of TMB in a sample of TMB-doped polymer ZEONOR (Figure S6).

Next, we monitor the charge separation from the intermediate triplet state by recording TA spectra on the time scale from milliseconds to seconds (Figure 4). Panels A

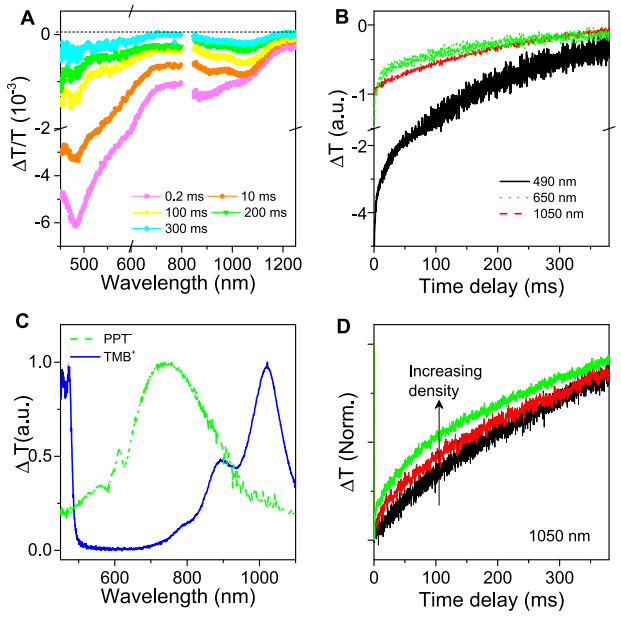

Figure 4. Charge separation and diffusion dynamics on the millisecond time scale. (A) Millisecond-resolved TA spectra at different time delays. (B) Millisecond-resolved kinetics probed at different wavelengths for a 10 mol % TMB/PPT film. (C) Absorption spectra of PPT^{-} and TMB^{+} characterized by spectroelectrochemistry measurements. (D) Normalized kinetic curves probed at 1050 nm under different excitation densities of 12, 48, and 96 μJ/cm^2. The pump wavelength was 355 nm.

and B of Figure 4 show the TA spectra recorded at different time delays and the kinetic curves probed at different wavelengths, respectively. The decay dynamics strongly depends on the probe wavelength because of the involvement of different excited species, including ^{3}CT, ^{3}LE, TMB^{+}, and PPT^{-}. To further analyze these different species, we record the spectral features of TMB^{+} and PPT^{-} by spectroelectrochem-

https://dx.doi.org/10.1021/acs.jpclett.0c00880
J. Phys. Chem. Lett. 2020, 11, 3582−3588

istry experiments (Figure 4C; see Figure S7 for details). The absorption features of TMB^+ appear in the infrared band centered at ~1050 nm and at wavelengths shorter than 500 nm, while the absorption of PPT^- consists of a broadband response centered at 750 nm (Figure 4C). Because the absorption of intermediate triplets is in the short-wavelength range centered at 490 nm, the signals probed at 1050 and 650 nm are mainly caused by TMB^+ and PPT^-, respectively. The signal probed at 650 nm decays much faster than that probed at 1050 nm, which is probably caused by the unbalanced diffusion of PPT^- and TMB^+ in the blend films. Because the TMB molecules are dispersed randomly and discretely in the PPT matrix, it is reasonable that the diffusion of TMB^+ is much less efficient than that of PPT^-. The remaining concentration of TMB^+ at the probed spot will be considerably higher than that of PPT^- at a late stage (Figure 4A). Such a scenario is further confirmed by temperature-dependent measurements. When the temperature decreases, the diffusion of PPT^- slows and the signal of TMB^+ is less pronounced (Figure S8).

The presence of CS states is also supported by the results of power-dependent measurements (Figure 4D), in which the decay rate increases with an increase in excitation density because of the bimolecular recombination of free charges. In contrast, the power dependence was not observed on the submicrosecond time scale, confirming the charge separation occurs after the ISC process. The observation of different diffusion properties of TMB^+ and PPT^- provides evidence of the involvement of ^{3}CT states (i.e., the bounded states of TMB^+ and PPT^-) in the triplet intermediates because PPT^- cannot be directly generated from ^{3}LE states at TMB. The dissociation of ^{3}CT states induces the charge separation and shifts the equilibrium between ^{3}CT and ^{3}LE states. In addition to charge generation, the phosphorescent emission and reverse ISC processes also lead to the decay of the triplet population,[36−38] which cause simultaneous removal of TMB^+ and PPT^-. The CS state formed by unbalanced charge diffusion contributes to the observed LPL when the PPT^- encounters TMB^+ in the probed spot through the fluorescence emission from the ^{1}CT states or the phosphorescence emission from the ^{3}CT and ^{3}LE states. The channels for LPL and phosphorescent emission are thus highly sensitive to the competition between carrier diffusion and recombination of ^{3}LE states.

To verify the model proposed above, we compare the temperature dependence of LPL emission in the blend film with that of the phosphorescence emission from the ^{3}LE state of TMB in a sample of TMB-doped polymer ZEONOR. If the triplet intermediates consist of mixed ^{3}LE and ^{3}CT states, their relative weights should vary with the environmental temperature. Considering that the ^{3}LE state is slightly lower in energy than the ^{3}CT state (Figure 3B), the triplet intermediates should contain a larger contribution from the ^{3}LE (^{3}CT) state at a lower (higher) temperature.

We check this assessment by measuring the temperature-dependent light emission from the intermediate triplet state of the blend film (Figure 5). As shown in Figure 5A, in addition to the LPL component with dynamics following the Debye−Edwards law (t^{-1} decay profile),[27,39,40] an exponential decay component becomes substantial on the time scale of <10 s when the temperature decreases (Figure S9). The exponential decay component can be assigned to the phosphorescence emission from the intermediate triplet state, whereas the decay dynamics is similar to the phosphorescence emission from the

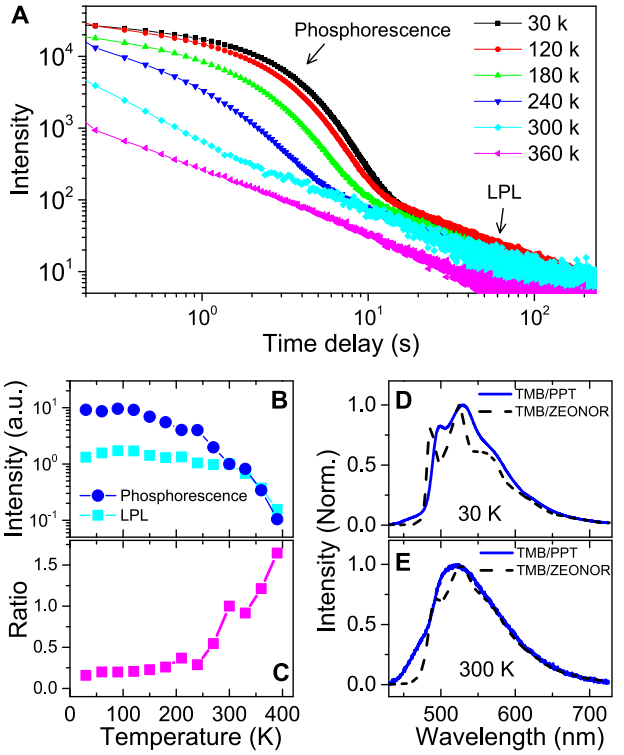

Figure 5. Temperature dependence of LPL of a TMB/PPT blend film. (A) Double logarithmic plot of the emission decay profile of a 10 mol % TMB/PTT film at different temperatures. (B) Temperature dependencies of emission intensities integrated over 0.1−1 s (phosphorescence) and 20−100 s (LPL) for the same blend film, respectively. (C) Intensity ratio of LPL to phosphorescence emissions plotted vs temperature. The values in panels B and C are normalized to the values recorded at 300 K. Phosphorescence spectra of the blend film measured at (D) 30 and (E) 300 K compared with those of a TMB/ZEONOR sample.

^{3}LE state of TMB (Figure S9). Avoiding the overlap time range (1−20 s), we compare the temperature dependences of the phosphorescence (integration from 0.1 to 1 s) and LPL (integration from 20 to 100 s) emissions in panels B and C of Figure 5. The intensity ratio between LPL and phosphorescence emission increases dramatically with an increase in temperature (Figure 5C), which supports the scenario of charge separation from ^{3}CT states in the blends. With an increase in temperature, the proportion of ^{3}CT states in the triplet intermediates increases and the rate of diffusion of PPT^- also increases, resulting in more efficient generation of CS states, which is responsible for the enhanced LPL emission. Nevertheless, the intensity of LPL decreases with an increase in temperature above 300 K, which is different from the temperature-dependent LPL in the inorganic systems.

The phosphorescence emission spectra from the TMB/PPT blend film are also dependent on temperature (Figure 5D,E and Figure S9). At 30 K, the phosphorescence from the blend exhibits a structured spectrum (Figure 5D), which is consistent with the higher relative proportion of the ^{3}LE state because the vibrational progression is mainly caused by the pure LE state.[41] The emission spectrum becomes less structured at room temperature, which is related to the line width broadening and energy distribution over different energy levels (Figure 5E). Notably, vibronic features can be observed in the emission spectrum from the TMB/ZEONOR blend film. Such a

https://dx.doi.org/10.1021/acs.jpclett.0c00880
J. Phys. Chem. Lett. 2020, 11, 3582−3588

difference confirms an important contribution of ^{3}CT states to the phosphorescence emission in the TMB/PPT blends at room temperature. In organic guest/host systems, exciplex states due to hybridization of LE and CT states may result in thermally activated delayed fluorescence.[42−44] Such an exciplex emission is possibly involved in the exponential decay component of light emission in the TMB/PPT system that is not invovled in the LPL emission.[45]

Previously, it has been suggested that the triplet exciplex states with mixed ^{3}CT and ^{3}LE characters may also be formed at the organic donor/acceptor interfaces.[41,46] However, this is unlikely to be the major channel here because the ratio between the signals of ^{3}CT and ^{3}LE states varies considerably with a change in temperature, which is also consistent with the recently identified effect of the energy gap between the LE and CT states on LPL.[45] The temperature dependences of phosphorescence and LPL emissions strongly support the involvement of mixed ^{3}CT and ^{3}LE states in the organic guest/host system. On the basis of the experimental evidence presented above, the carrier dynamics responsible for the LPL emission in the TMB/PPT blends can be illustrated as shown in Figure 1A. The long-lived ^{3}LE states allow relatively efficient ISC from ^{1}CT states, whereas the ^{3}CT states enable charge separation because of the unbalanced diffusion of cations and anions. The mixed ^{3}LE/^{3}CT states connected the photoexcited singlet states to the long-lived CS states. The decay dynamics of CS states become faster with an increase in the doping level of TMB due to the enhanced encountering probability of charge-separated radicals. The CS states act like the trapping states in inorganic LPL systems.[47] To some extent, the mixed ^{3}LE/^{3}CT states behave like the stabilized triplet excited state, providing ultralong phosphorescence in neat organic crystals.[8,21] The donor/acceptor interfaces in which the ^{3}CT state dissociates into the CS state for LPL in the TMB/PPT blend are absent in the neat systems. Moreover, the diffusion properties are likely very different for these different excited species. To fully understand these effects, more in-depth kinetic modeling,[48] combined with time-resolved and spatially resolved approaches, will be necessary in the future. These insights imply that highly efficient LPL may become achievable in organic co-crystals of donor/acceptor systems.[49,50]

In summary, we have identified the key triplet intermediates of mixed ^{3}LE and ^{3}CT states responsible for LPL in the TMB/PPT blend films. The triplet intermediates generated through the ISC process from the ^{1}CT state are long-lived, allowing efficient carrier diffusion to dissociate the ^{3}CT states into the CS state for LPL emission. Future study with time-resolved ESR measurements may provide more insights into the dynamics of triplet excited states involved in the generation of LPL. The mechanism uncovered in this work may guide the search for new organic guest/host combinations with high-performance LPL emission. More importantly, the identification of a long-lived triplet channel for charge separation suggests an alternative strategy for designing organic architectures for a variety of optoelectronic applications relying on photon-to-charge conversion.

■ ASSOCIATED CONTENT

Supporting Information

The Supporting Information is available free of charge at https://pubs.acs.org/doi/10.1021/acs.jpclett.0c00880.

Materials and methods, control TA measurements of charge dynamics, quantum computational results, spectro-electrochemistry measurements, and temperature-dependent measurements (PDF)

■ AUTHOR INFORMATION

Corresponding Author

Chunfeng Zhang − *National Laboratory of Solid State Microstructures, School of Physics, and Collaborative Innovation Center for Advanced Microstructures, Nanjing University, Nanjing 210093, China;* orcid.org/0000-0001-9030-5606; Email: cfzhang@nju.edu.cn

Authors

Leixin Xiao − *National Laboratory of Solid State Microstructures, School of Physics, and Collaborative Innovation Center for Advanced Microstructures, Nanjing University, Nanjing 210093, China*

Zhiwei Wang − *National Laboratory of Solid State Microstructures, School of Physics, and Collaborative Innovation Center for Advanced Microstructures, Nanjing University, Nanjing 210093, China*

Xiaoyu Xie − *School of Chemistry and Chemical Engineering, Nanjing University, Nanjing 210093, China*

Haibo Ma − *School of Chemistry and Chemical Engineering, Nanjing University, Nanjing 210093, China;* orcid.org/0000-0001-7915-3429

Qian Peng − *China Key Laboratory of Organic Solids and Beijing National Laboratory for Molecular Science, Institute of Chemistry, Chinese Academy of Sciences, Beijing 100190, China;* orcid.org/0000-0001-8975-8413

Zhongfu An − *Key Laboratory of Flexible Electronics and Institute of Advanced Materials, Nanjing Tech University, Nanjing 211816, China;* orcid.org/0000-0002-6522-2654

Xiaoyong Wang − *National Laboratory of Solid State Microstructures, School of Physics, and Collaborative Innovation Center for Advanced Microstructures, Nanjing University, Nanjing 210093, China;* orcid.org/0000-0003-1147-0051

Zhigang Shuai − *Department of Chemistry and MOE Key Laboratory of Organic Optoelectronics and Molecular Engineering, Tsinghua University, Beijing 10084, China;* orcid.org/0000-0003-3867-2331

Min Xiao − *National Laboratory of Solid State Microstructures, School of Physics, and Collaborative Innovation Center for Advanced Microstructures, Nanjing University, Nanjing 210093, China; Department of Physics, University of Arkansas, Fayetteville, Arkansas 72701, United States*

Complete contact information is available at: https://pubs.acs.org/10.1021/acs.jpclett.0c00880

Author Contributions

[@]L.X. and Z.W. contributed equally to this work.

Notes

The authors declare no competing financial interest.

■ ACKNOWLEDGMENTS

This work was supported by the National Key R&D Program of China (2018YFA0209100 and 2017YFA0303703), the National Natural Science Foundation of China (21922302, 21873047, 11574140, 91850105, 91833305, and 11621091), the Priority Academic Program Development of Jiangsu Higher Education Institutions (PAPD), and the Fundamental

Research Funds for the Central Universities. C.Z. acknowledges financial support from the Tang Scholar program.

REFERENCES

(1) Baldo, M. A.; O'Brien, D. F.; You, Y.; Shoustikov, A.; Sibley, S.; Thompson, M. E.; Forrest, S. R. Highly efficient phosphorescent emission from organic electroluminescent devices. *Nature* **1998**, *395* (6698), 151−154.
(2) Li, Y.; Gecevicius, M.; Qiu, J. Long persistent phosphors-from fundamentals to applications. *Chem. Soc. Rev.* **2016**, *45* (8), 2090−2136.
(3) Zhao, Q.; Huang, C.; Li, F. Phosphorescent heavy-metal complexes for bioimaging. *Chem. Soc. Rev.* **2011**, *40* (5), 2508−2524.
(4) Zhang, G.; Palmer, G. M.; Dewhirst, M.; Fraser, C. L. A dual-emissive-materials design concept enables tumour hypoxia imaging. *Nat. Mater.* **2009**, *8* (9), 747−751.
(5) You, Y.; Lee, S.; Kim, T.; Ohkubo, K.; Chae, W.-S.; Fukuzumi, S.; Jhon, G.-J.; Nam, W.; Lippard, S. J. Phosphorescent sensor for biological mobile zinc. *J. Am. Chem. Soc.* **2011**, *133* (45), 18328−18342.
(6) Fermi, A.; Bergamini, G.; Roy, M.; Gingras, M.; Ceroni, P. Turn-on phosphorescence by metal coordination to a multivalent terpyridine ligand: A new paradigm for luminescent sensors. *J. Am. Chem. Soc.* **2014**, *136* (17), 6395−6400.
(7) Xu, J.; Tanabe, S. Persistent luminescence instead of phosphorescence: History, mechanism, and perspective. *J. Lumin.* **2019**, *205*, 581−620.
(8) An, Z. F.; Zheng, C.; Tao, Y.; Chen, R. F.; Shi, H. F.; Chen, T.; Wang, Z. X.; Li, H. H.; Deng, R. R.; Liu, X. G.; Huang, W. Stabilizing triplet excited states for ultralong organic phosphorescence. *Nat. Mater.* **2015**, *14* (7), 685−690.
(9) Zhang, X.; Du, L.; Zhao, W.; Zhao, Z.; Xiong, Y.; He, X.; Gao, P. F.; Alam, P.; Wang, C.; Li, Z.; Leng, J.; Liu, J.; Zhou, C.; Lam, J. W. Y.; Phillips, D. L.; Zhang, G.; Tang, B. Z. Ultralong UV/mechano-excited room temperature phosphorescence from purely organic cluster excitons. *Nat. Commun.* **2019**, *10*, 5161.
(10) Wang, Z.; Zhang, Y.; Wang, C.; Zheng, X.; Zheng, Y.; Gao, L.; Yang, C.; Li, Y.; Qu, L.; Zhao, Y. Color-tunable polymeric long-persistent luminescence based on polyphosphazenes. *Adv. Mater.* **2020**, *32* (7), 1907355.
(11) Narushima, K.; Kiyota, Y.; Mori, T.; Hirata, S.; Vacha, M. Suppressed triplet exciton diffusion due to small orbital overlap as a key design factor for ultralong-lived room-temperature phosphorescence in molecular crystals. *Adv. Mater.* **2019**, *31* (10), 1807268.
(12) Louis, M.; Thomas, H.; Gmelch, M.; Haft, A.; Fries, F.; Reineke, S. Blue-light-absorbing thin films showing ultralong room-temperature phosphorescence. *Adv. Mater.* **2019**, *31* (12), 1807887.
(13) Tao, Y.; Chen, R.; Li, H.; Yuan, J.; Wan, Y.; Jiang, H.; Chen, C.; Si, Y.; Zheng, C.; Yang, B.; Xing, G.; Huang, W. Resonance-activated spin-flipping for efficient organic ultralong room-temperature phosphorescence. *Adv. Mater.* **2018**, *30* (44), 1803856.
(14) Zhen, X.; Tao, Y.; An, Z.; Chen, P.; Xu, C.; Chen, R.; Huang, W.; Pu, K. Ultralong phosphorescence of water-soluble organic nanoparticles for in vivo afterglow imaging. *Adv. Mater.* **2017**, *29* (33), 1606665.
(15) Cai, S.; Shi, H.; Li, J.; Gu, L.; Ni, Y.; Cheng, Z.; Wang, S.; Xiong, W.-w.; Li, L.; An, Z.; Huang, W. Visible-light-excited ultralong organic phosphorescence by manipulating intermolecular interactions. *Adv. Mater.* **2017**, *29* (35), 1701244.
(16) Ma, X.; Xu, C.; Wang, J.; Tian, H. Amorphous pure organic polymers for heavy-atom-free efficient room-temperature phosphorescence emission. *Angew. Chem., Int. Ed.* **2018**, *57* (34), 10854−10858.
(17) Bian, L.; Shi, H.; Wang, X.; Ling, K.; Ma, H.; Li, M.; Cheng, Z.; Ma, C.; Cai, S.; Wu, Q.; Gan, N.; Xu, X.; An, Z.; Huang, W. Simultaneously enhancing efficiency and lifetime of ultralong organic phosphorescence materials by molecular self-assembly. *J. Am. Chem. Soc.* **2018**, *140* (34), 10734−10739.
(18) Yang, J.; Zhen, X.; Wang, B.; Gao, X.; Ren, Z.; Wang, J.; Xie, Y.; Li, J.; Peng, Q.; Pu, K.; Li, Z. The influence of the molecular packing on the room temperature phosphorescence of purely organic luminogens. *Nat. Commun.* **2018**, *9*, 840.
(19) Wang, J.; Gu, X.; Ma, H.; Peng, Q.; Huang, X.; Zheng, X.; Sung, S. H. P.; Shan, G.; Lam, J. W. Y.; Shuai, Z.; Tang, B. Z. A facile strategy for realizing room temperature phosphorescence and single molecule white light emission. *Nat. Commun.* **2018**, *9*, 2963.
(20) Shoji, Y.; Ikabata, Y.; Wang, Q.; Nemoto, D.; Sakamoto, A.; Tanaka, N.; Seino, J.; Nakai, H.; Fukushima, T. Unveiling a new aspect of simple arylboronic esters: Long-lived room-temperature phosphorescence from heavy-atom-free molecules. *J. Am. Chem. Soc.* **2017**, *139* (7), 2728−2733.
(21) Ma, H.; Peng, Q.; An, Z. F.; Huang, W.; Shuai, Z. Efficient and long-lived room-temperature organic phosphorescence: Theoretical descriptors for molecular designs. *J. Am. Chem. Soc.* **2019**, *141*, 1010−1015.
(22) Wei, J.; Liang, B.; Duan, R.; Cheng, Z.; Li, C.; Zhou, T.; Yi, Y.; Wang, Y. Induction of strong long-lived room-temperature phosphorescence of N-Phenyl-2-naphthylamine molecules by confinement in a crystalline dibromobiphenyl matrix. *Angew. Chem., Int. Ed.* **2016**, *55* (50), 15589−15593.
(23) Gu, L.; Shi, H.; Gu, M.; Ling, K.; Ma, H.; Cai, S.; Song, L.; Ma, C.; Li, H.; Xing, G.; Hang, X.; Li, J.; Gao, Y.; Yao, W.; Shuai, Z.; An, Z.; Liu, X.; Huang, W. Dynamic ultralong organic phosphorescence by photoactivation. *Angew. Chem., Int. Ed.* **2018**, *57* (28), 8425−8431.
(24) Hirata, S. Recent ddvances in materials with room-temperature phosphorescence: Photophysics for triplet exciton stabilization. *Adv. Opt. Mater.* **2017**, *5* (17), 1700116.
(25) Ogoshi, T.; Tsuchida, H.; Kakuta, T.; Yamagishi, T.-a.; Taema, A.; Ono, T.; Sugimoto, M.; Mizuno, M. Ultralong room-temperature phosphorescence from amorphous polymer poly(styrene sulfonic acid) in air in the dry solid state. *Adv. Funct. Mater.* **2018**, *28* (16), 1707369.
(26) Al-Attar, H. A.; Monkman, A. P. Room-temperature phosphorescence from films of isolated water-soluble conjugated polymers in hydrogen-bonded matrices. *Adv. Funct. Mater.* **2012**, *22* (18), 3824−3832.
(27) Kabe, R.; Adachi, C. Organic long persistent luminescence. *Nature* **2017**, *550* (7676), 384−387.
(28) Alam, P.; Leung, N.; Liu, J.; Zhang, X.; He, Z.; Kwok, R. T. K.; Lam, J. W. Y.; Sung, H. H.-Y.; Williams, I. D.; Peng, Q.; Tang, B. Z. Two are better than one: A design principle for ultralong persistent luminescence of pure organics. *ChemRxiv* **2019**, DOI: 10.26434/chemrxiv.8298839.v1.
(29) Lin, Z. S.; Kabe, R.; Nishimura, N.; Jinnai, K.; Adachi, C. Organic long-persistent luminescence from a flexible and transparent doped polymer. *Adv. Mater.* **2018**, *30* (45), 1803713.
(30) Clarke, T. M.; Durrant, J. R. Charge photogeneration in organic solar cells. *Chem. Rev.* **2010**, *110* (11), 6736−6767.
(31) Guo, J.; Togami, T.; Benten, H.; Ohkita, H.; Ito, S. Simultaneous multi-photon ionization of aromatic molecules in polymer solids with ultrashort pulsed lasers. *Chem. Phys. Lett.* **2009**, *475* (4−6), 240−244.
(32) Wasserman, E.; Yager, W. A.; Snyder, L. C. ESR of triplet states of randomly oriented molecules. *J. Chem. Phys.* **1964**, *41* (6), 1763−1772.
(33) Nakanotani, H.; Furukawa, T.; Morimoto, K.; Adachi, C. Long-range coupling of electron-hole pairs in spatially separated organic donor-acceptor layers. *Sci. Adv.* **2016**, *2* (2), No. e1501470.
(34) Elsayed, M. A. Spin-orbit coupling and radiationless processes in nitrogen heterocyclics. *J. Chem. Phys.* **1963**, *38* (12), 2834−2838.
(35) Gould, I. R.; Boiani, J. A.; Gaillard, E. B.; Goodman, J. L.; Farid, S. Intersystem crossing in charge-transfer excited states. *J. Phys. Chem. A* **2003**, *107* (18), 3515−3524.
(36) Yang, Z.; Mao, Z.; Xie, Z.; Zhang, Y.; Liu, S.; Zhao, J.; Xu, J.; Chi, Z.; Aldred, M. P. Recent advances in organic thermally activated delayed fluorescence materials. *Chem. Soc. Rev.* **2017**, *46* (3), 915−1016.

https://dx.doi.org/10.1021/acs.jpclett.0c00880
J. Phys. Chem. Lett. 2020, 11, 3582−3588

(37) Goushi, K.; Yoshida, K.; Sato, K.; Adachi, C. Organic light-emitting diodes employing efficient reverse intersystem crossing for triplet-to-singlet state conversion. *Nat. Photonics* **2012**, *6* (4), 253−258.
(38) Noda, H.; Nakanotani, H.; Adachi, C. Excited state engineering for efficient reverse intersystem crossing. *Sci. Adv.* **2018**, *4* (6), No. eaao6910.
(39) Debye, P.; Edwards, J. O. Long-lifetine phosphorescence and the diffusion process. *J. Chem. Phys.* **1952**, *20* (2), 236−239.
(40) Hamill, W. H. Debye-Edwards electron recombination kinetics. *J. Chem. Phys.* **1979**, *71* (1), 140−142.
(41) Yersin, H. *Highly efficient OLEDs: Materials based on thermally activated delayed fluorescence*, 1st ed.; Wiley-VCH: Weinheim, Germany, 2019; Vol. *10*, pp 331−376.
(42) Sarma, M.; Wong, K.-T. Exciplex: An intermolecular charge-transfer approach for TADF. *ACS Appl. Mater. Interfaces* **2018**, *10* (23), 19279−19304.
(43) Jinnai, K.; Nishimura, N.; Kabe, R.; Adachi, C. Fabrication-method independence of organic long-persistent luminescence performance. *Chem. Lett.* **2019**, *48* (3), 270−273.
(44) Deng, C.; Zhang, L.; Wang, D.; Tsuboi, T.; Zhang, Q. Exciton- and polaron-induced reversible dipole reorientation in amorphous organic semiconductor films. *Adv. Opt. Mater.* **2019**, *7* (8), 1801644.
(45) Lin, Z.; Kabe, R.; Wang, K.; Adachi, C. Influence of energy gap between charge-transfer and locally excited states on organic long persistence luminescence. *Nat. Commun.* **2020**, *11* (1), 191.
(46) Lin, T.-C.; Sarma, M.; Chen, Y.-T.; Liu, S.-H.; Lin, K.-T.; Chiang, P.-Y.; Chuang, W.-T.; Liu, Y.-C.; Hsu, H.-F.; Hung, W.-Y.; Tang, W.-C.; Wong, K.-T.; Chou, P.-T. Probe exciplex structure of highly efficient thermally activated delayed fluorescence organic light emitting diodes. *Nat. Commun.* **2018**, *9*, 3111.
(47) Pan, Z.; Lu, Y.-Y.; Liu, F. Sunlight-activated long-persistent luminescence in the near-infrared from Cr^{3+}-doped zinc gallogermanates. *Nat. Mater.* **2012**, *11* (1), 58−63.
(48) Gopich, I. V.; Solntsev, K. M.; Agmon, N. Excited-state reversible geminate reaction. I. Two different lifetimes. *J. Chem. Phys.* **1999**, *110* (4), 2164−2174.
(49) Sun, L.; Zhu, W.; Yang, F.; Li, B.; Ren, X.; Zhang, X.; Hu, W. Molecular cocrystals: design, charge-transfer and optoelectronic functionality. *Phys. Chem. Chem. Phys.* **2018**, *20* (9), 6009−6023.
(50) Zhang, J.; Xu, W.; Sheng, P.; Zhao, G. Y.; Zhu, D. B. Organic donor-acceptor complexes as novel organic semiconductors. *Acc. Chem. Res.* **2017**, *50* (7), 1654−1662.

https://dx.doi.org/10.1021/acs.jpclett.0c00880
J. Phys. Chem. Lett. 2020, 11, 3582−3588